PHYSICAL REVIEW E **69**, 025401(R) (2004)

Terahertz radiation from the vacuum-plasma interface driven by ultrashort intense laser pulses

Zheng-Ming Sheng, Hui-Chun Wu, Kun Li, and Jie Zhang
Laboratory of Optical Physics, Institute of Physics, Chinese Academy of Science, Beijing 100080, China
(Received 5 November 2003; published 25 February 2004)

Coherent terahertz (THz) emission from the vacuum-plasma interface induced through laser wake-field excitation has been investigated by particle-in-cell simulations. The emission frequency appears around τ_L^{-1}, where τ_L is the laser pulse duration, even though the plasma density is distributed inhomogeneously near the interface. The emission amplitude, which is zero on the propagation axis of the incident pulse, increases transversely until reaching the maximum amplitude at the beam edge of the incident pulse and then decays transversely. The emission power scales like $P \sim 10^8 \times a_0^4$ W, where a_0 is the normalized field amplitude of the laser pulse. For an incident pulse of a few tens of femtoseconds at the forced intensity of 3×10^{17} W/cm^2, it can generate THz radiation with a power of a few MW and with an energy of several μJ/pulse.

DOI: 10.1103/PhysRevE.69.025401 PACS number(s): 52.35.Mw, 52.59.Ye, 52.65.Rr

Since terahertz (THz) radiation finds wide applications in sensing and imaging, etc., the topic of THz radiation generation has been attracting continued interest over the last decade. Among the various schemes for generating the THz waves, an important and direct way is to make use of femtosecond laser pulses interacting with different electro-optic crystals and semiconductors through optical rectification [1–3], since the bandwidth of such laser pulses is just around THz. Recently it has been suggested that THz emission can be generated from very short electron bunches bending in a magnetic field [4,5], traversing a medium with a discontinuous refractive index [6,7], or crossing a plasma-vacuum boundary [8]. On the other hand, plasma can serve as a unique medium for rectifying femtosecond pulses at various intensities to generate THz emission. The resulting emission can also serve as a useful diagnostic tool of the plasma state. At low light intensities, it is found that THz emission from laser interactions with plasmas can be produced by the photoionization of electrically biased air with femtosecond laser pulses [9]. At high light intensities, THz emission from intense femtosecond laser interaction with plasma was observed even ten years ago [10]. The rapidly established space-charge fields driven by the ponderomotive force of the laser pulse are responsible for the observed radiation. More recently, THz radiation emitted from formed filaments and plasma channels of an intense laser pulse propagating in air has been investigated experimentally [11] and theoretically [12]. It is suggested that the induced electron plasma oscillation is responsible for the emission. However, the proposed one-dimensional theory model is supposed to be insufficient to describe the radiation generation [13]. Up to now, a full understanding about the radiation generation through the plasma wave excitation is still not available.

In this paper, we present a numerical investigation of the generation of low frequency radiation around τ_L^{-1}, where τ_L is the laser pulse duration. The radiation caused by electron plasma oscillation is found to be due to the presence of a vacuum-plasma interface as well as a moderate plasma density inhomogeneity. When the local electron plasma frequency $\omega_p \sim 2\pi/\tau_L$, significant radiation can emit from plasma into vacuum.

A series of numerical simulations have been conducted using a two-dimensional (2D) particle-in-cell (PIC) code, which is developed following a scheme described in Ref. [14]. A transverse dimension proves to be essential to observe low-frequency emissions from the vacuum-plasma boundary. In a typical simulation, a plasma slab with either a homogeneous or inhomogeneous density profile is located in the center of the simulation box, which has a dimension of $200\lambda\times100\lambda$, with λ the laser wavelength in vacuum. The laser pulse has a sine-square longitudinal profile $a = a_0 \sin^2(\pi t/\tau_L)\exp(-y^2/2R^2)$ for $0 \leqslant t \leqslant \tau_L$, where a_0 is the normalized peak amplitude, τ_L the duration normalized by a laser cycle τ_0, and R the focused radius normalized by λ. It is incident from the left boundary of the simulation box. In order to distinguish clearly the induced low frequency emissions from the incident pulse, the incident pulse is *s* polarized with its electric component along the *z* direction and its magnetic component along the *y* direction. In the 2D geometry, the generated low-frequency radiation is *p* polarized, as shown below.

Figure 1 illustrates two typical simulations for different plasma density profiles at the vacuum-plasma interface. In case (I), the plasma density increases linearly from $0.0025n_c$ up to $0.01n_c$ in a length of 60λ, where n_c is the critical density of the incident pulse. In case (II), the plasma density increases exponentially from $0.002n_c$ up to $2n_c$ in a length of 80λ. Columns (I) and (II) in Fig. 1 represent the obtained simulation results for the two cases, respectively. The incident pulse is with a peak amplitude $a_0=0.5$, a duration $\tau_L = 20\tau_0$, and a focused radius $R=15\lambda$ for both cases. Shown in this figure are snapshots of the electron density profiles and the time-averaged (over a laser cycle of the incident pulse) longitudinal and transverse fields E_x, E_y, and B_z. In contrast to a plasma wave driven in infinite homogeneous plasma, the excited wake plasma wave in an inhomogeneous plasma evolves more complicatedly with time. This is because both the oscillation frequency and wavelength are space dependent. Note that a longitudinal electric field is found only inside the plasma, while transverse electric and magnetic fields are found both inside the plasma and outside in vacuum. In particular, the amplitude of the magnetic field is larger in vacuum than in the plasma. The fields in the

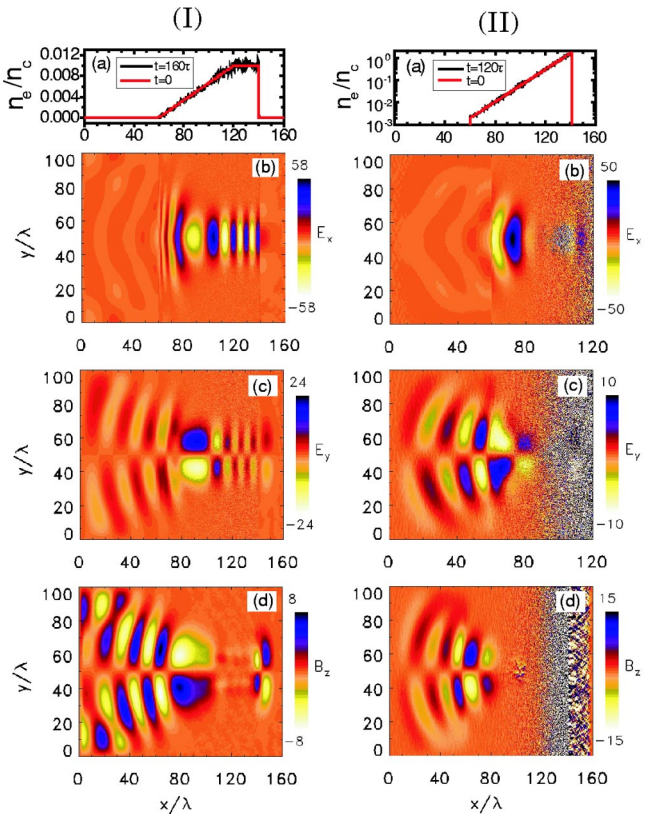

FIG. 1. (Color online) Snapshots showing the electron density profile (a), the excited longitudinal electric field E_x (b), the transverse electric field E_y (c), and the magnetic field B_z (d). These fields are time averaged over a laser cycle of the incident pulse. Column (I) is for the case with a linear plasma density profile, obtained at time $t=160\tau_0$ and column (II) is for the case with an exponential plasma density profile, obtained at time $t=120\tau_0$. The electric and magnetic fields are normalized by $m\omega_0 c/e$ and multiplied by a factor of 10^4 in the scale bar. In both cases, the incident pulse has a duration of $20\tau_0$, a focused radius $R=15\lambda$, and a peak amplitude $a_0=0.5$.

vacuum region are the electromagnetic wave emitted from the plasma. In both cases, we observe that the radiation amplitude $eB_z/m\omega_0 c \sim eE_y/m\omega_0 c \approx 10^{-3}$ in vacuum, which exceeds 3×10^7 V/cm for the electric field. One notes that the emission amplitude is peaked at the beam edge of the incident pulse and vanishes along the beam axis. The latter suggests that the induced radiation is proportional to the transverse derivation of laser intensity da_0^{ϵ}/dr, i.e., inversely proportional to the focused radius R. Here $\epsilon>0$ is a coefficient, which is found to be about 2, as shown later. In addition, the induced radiation appears to emit in a narrow conical structure from its source at the vacuum-plasma boundary. Because of the transverse symmetry of the ponderomotive force in tenuous plasma, the induced electric field should point in the radial direction and the magnetic field in the azimuthal direction in a three-dimensional geometry.

Figure 2(a) shows the time evolution of the induced low-frequency electromagnetic field through the left boundary of the simulation box at $y=60\lambda$ (away from the propagation axis at $y=50\lambda$) for the two cases. Note that for case (I) the

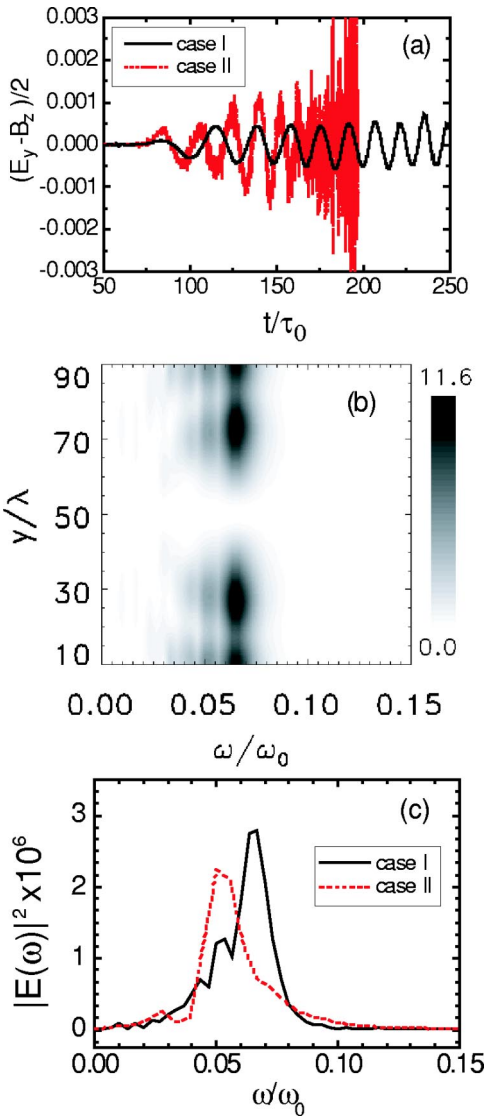

FIG. 2. (Color online) (a) Time dependent field (normalized by $m\omega_0 c/e$) emitted through the left boundary of the simulation box at $y=60\lambda$ obtained for both cases (I) and (II) indicated in Fig. 1. (b) Emission spectrum through the left boundary of the simulation box obtained for case (I) with a linear density profile, where the scale bar is in arbitrary units. (c) Total emission spectra by summing over the grid points in transverse (y) direction for both cases (I) and (II).

low-frequency radiation lasts for a long time over 200 laser cycles. For case (II), when the maximum target density is overcritical, the induced radiation can be distinguished only within the first 100 laser cycles, beyond which it is submerged in the noise. In both cases, the radiation frequency appears to increase with time. This originates from the plasma inhomogeneity at the boundary, where the electron plasma frequency increases as away from the vacuum-plasma interface. Therefore, the high frequency in the radiation appears at later time. Figure 2(b) shows the emission spectrum distribution in the ω-y space. It shows that obviously there is no emission on the propagation axis. Figure 2(c) shows the total emission spectra (by summing over all the transverse grid points) through the left boundary of the

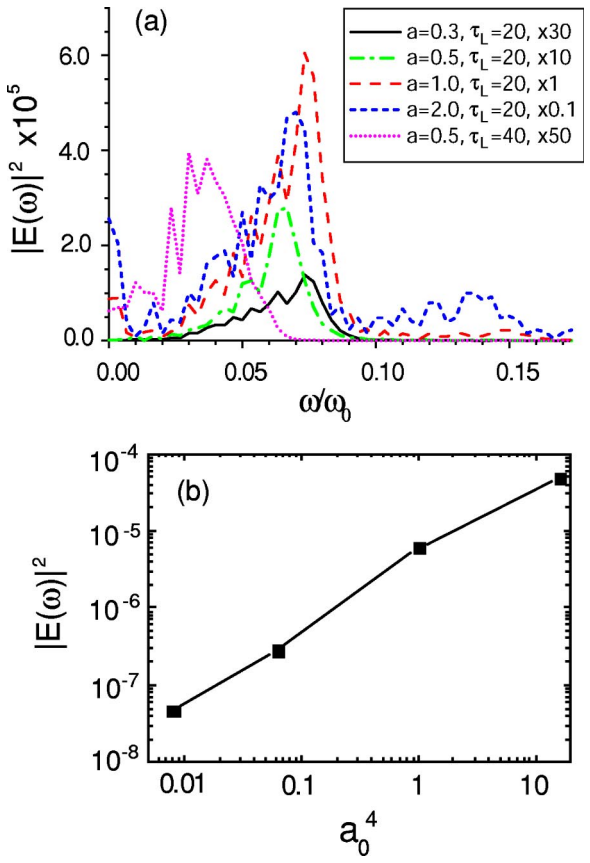

FIG. 3. (Color online) (a) Emission spectra obtained for various laser intensities and pulse durations of the incident laser pulse, which have been multiplied by different numerical factors for different laser intensities. The corresponding plasma density profile is the same as the case (I) shown in Fig. 1. (b) The emission spectrum peaks as a function of the pulse peak amplitudes for a fixed pulse duration and plasma density profile.

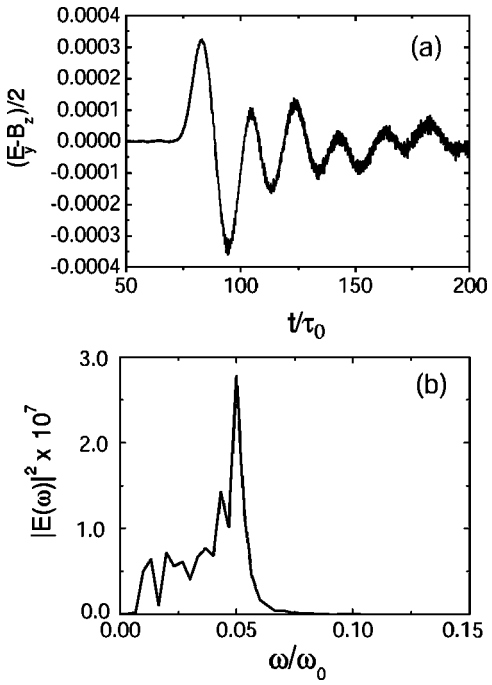

FIG. 4. (a) Time dependence of the induced emission when the initial plasma slab has a sharp boundary and a fixed density at $n_0/n_c=0.0025$. (b) Total emission spectrum obtained by summing over transverse grid points. The incident pulse has a peak amplitude $a_0=0.5$, a duration $\tau_L=20\tau_0$, and a focused radius $R=15\lambda$.

simulation box. For case (I) the spectrum is peaked around $0.065\omega_0$, while for case (II) the corresponding spectrum is peaked around $0.05\omega_0$. We mention that there is also a forward emission at the right plasma-vacuum boundary induced when the laser pulse propagates through it. However, it is much weaker than the backward emission, as we see at the left vacuum-plasma boundary.

In another simulation, we increase the pulse duration to $\tau_L=40\tau_0$ while fixing the incident pulse intensity and the plasma density profile as in case (I) in Fig. 1. The emission frequency is now found to be near $0.035\omega_0$, i.e., close to $\omega_0/\tau_L=0.025\omega_0$, as shown in Fig. 3(a). The emission amplitude is comparable to that given in last examples, i.e., we have not seen much decrease in the radiation amplitude from that for $\tau_L=20\tau_0$. In other simulations, we change the pulse amplitudes while keeping the pulse duration at $\tau_L=20\tau_0$ and the plasma density profile. We find that the emission frequencies are all nearly at $0.06\omega_0$, as shown in Fig. 3(a). But the emission intensity depend strongly on the incident laser intensity. For $a_0=1$, for example, the emission amplitude is increased up to $eB_z/m\omega_0 c\approx 4\times 10^{-3}$, which is more than four times larger than that for $a_0=0.5$. From these simulations, and accounting for the fact that the induced emission amplitude is proportional to $1/R$, as mentioned before, we find that the emission amplitude scales with the amplitude and the transverse spot size of the laser pulse like $eB_z/m\omega_0 c\approx 0.05a_0^2/R$, which depends weakly on the pulse duration τ_L. Based on Fig. 3(a), the emission power through the left boundary is found to be approximately proportional to a_0^4, as shown in Fig. 3(b).

In an inhomogeneous plasma, the central frequency of the induced radiation is $\omega_{IR}\sim\omega_0/\tau_L$ and the corresponding wavelength is $\lambda_{IR}\sim\tau_L\lambda$, where τ_L is normalized by τ_0. Taking case (I) in Fig. 1 for the emission frequency $\omega=0.065\omega_0$ and the emission amplitude $eB_z/m\omega_0 c=0.001$, we find the intensity of emitted wave $I_{IR}\lambda_{IR}^2=3.2\times 10^{14}$ W/cm^2 μm^2. The corresponding emission power is 9.6×10^6 W if taking a beam diameter of 30 μm. The total emission energy depends upon the emitting pulse duration. The latter depends upon the lifetime of the excited plasma wave, which is related to the electron-ion collision frequency. For a lifetime of 1 ps, one finds the emission energy is about 10 μJ/pulse. Currently this is among the most powerful THz radiation sources. Generally, the radiation intensity and power can be expressed, respectively, as

$$I_{IR}\lambda_{IR}^2\sim a_0^4(\tau_L/R)^2\times(3\times 10^{15}\ \text{W/cm}^2\ \mu\text{m}^2),$$

$$P_{IR}\sim a_0^4\times 10^8\ \text{W}. \qquad (1)$$

Note that the emission power depends only upon the incident pulse intensity, and very weakly on the plasma density and emission frequency. However, a plasma density profile

with a different density scale length at the boundary may modify this scaling by some factors. If substituting $a_0^2 = 23.2(E_j\lambda^2/\tau_L R^2)$, where E_j is the pulse energy in Joule, λ, and R in μm, and τ_L in picoseconds, one finds from Eq. (1) that $P_{IR}=54(E_j\lambda^2/\tau_L R^2)^2$ GW. This power scaling is proportional to the square of the incident pulse energy, in agreement with that obtained by Hamster *et al.* [10]. But the scaling with pulse duration τ_L and the focused beam radius R is different from theirs. In their simplified calculations, the low frequency radiation is supposed to result from a linearly driven harmonic oscillator under the push of the laser ponderomotive force.

We also simulate the low frequency emission for the case when the plasma slab is homogeneous. Figure 4 shows the result for the plasma density at $n_0/n_c=0.0025$. It is found that the induced radiation is found with only a few cycles of oscillation, and then decays very quickly, as shown in Fig. 4(a). Meanwhile, the spectrum is relatively peaked around the plasma oscillation frequency $\omega_p=0.05\omega_0$ as shown in Fig. 4(b). However, the radiation generation with a sharp vacuum-plasma boundary is not as efficient as that from with a moderate scale length of the plasma density.

At present, there is no theory available dealing with the plasma wave excitation at the vacuum-plasma boundary in at least a two-dimensional geometry. Quasistatic magnetic field generation in infinite plasma has been studied recently in several publications [15,16]. According to these theories, the quasistatic magnetic field in a homogeneous plasma is proportional to da_0^4/dr for $a_0 \ll 1$ and da_0^2/dr for $a_0 \gg 1$. Obviously, this scaling does not apply to the present case for induced radiation. Meanwhile, the predicted magnetic field has two components. One is constant and independent of time. The other is nearly twice the plasma frequency. As a result, these theories cannot explain the induced radiation observed in our simulations. In another related work, electromagnetic emissions close to the plasma frequency and multiples of the plasma frequency have been observed both in simulations and experiments from femtosecond pulse interaction with solids [17]. Qualitatively, such radiation is supposed to be generated by a two-step process in which hot electron jets excite Langmuir waves in the overdense region, which then undergo parametric conversion to electromagnetic emission at harmonics of the plasma frequency. This is obviously different from our case.

In conclusion, strong low frequency radiations at a frequency around the inverse of the driving pulse duration from a vacuum-plasma interface have been observed in 2D PIC simulations. The radiations result from the excited large-amplitude plasma waves at the plasma boundary. For the incident pulse at 3×10^{17} W/cm^2, the induced emission can as large as MW in the power and a few μJ in the energy. It is found that a modest density scale length around the plasma boundary is favorable in producing induced emissions. This kind of density profile can be produced by launching a laser pulse transversely into a gas jet directly, or by launching a prepulse and a suitable delayed main pulse when a solid target is used.

This work was supported in part by the National Natural Science Foundation of China (Grant Nos. 10105014 and 10075075), the National High-Tech ICF Committee in China, the National Key Basic Research Special Foundation (NKBRSF) under Grant No. G1999075200.

[1] X.-C. Zhang, B.B. Hu, J.T. Darrow, and D.H. Auston, Appl. Phys. Lett. **56**, 1011 (1990).
[2] X.-C. Zhang, X.F. Ma, Y. Jin, T.-M. Lu, E.P. Boden, P.D. Phelps, K.R. Stewart, and C.P. Yakymyshyn, Appl. Phys. Lett. **61**, 3080 (1992).
[3] R. Kersting, K. Unterrainer, G. Strasser, H.F. Kauffmann, and E. Gornik, Phys. Rev. Lett. **79**, 3038 (1997).
[4] G.L. Carr, M.C. Martin, W.R. McKinney, K. Jordan, G.R. Neil, and G.P. Williams, Nature (London) **420**, 153 (2002).
[5] M. Abo-Bakr, J. Feikes, K. Holldack, P. Kuske, W.B. Peatman, U. Schade, G. Wuestefeld, and H.-W. Huebers, Phys. Rev. Lett. **90**, 094801 (2003).
[6] U. Happek *et al.*, Phys. Rev. Lett. **67**, 2962 (1991).
[7] D. Hashimshony, A. Zigler, and K. Papadopoulos, Phys. Rev. Lett. **86**, 2806 (2001).
[8] W.P. Leemans *et al.*, Phys. Rev. Lett. **91**, 074802 (2003).
[9] T. Löffler and H.G. Roskos, J. Appl. Phys. **91**, 2611 (2002).
[10] H. Hamster, A. Sullivan, S. Gordon, W. White, and R.W. Falcone, Phys. Rev. Lett. **71**, 2725 (1993); Phys. Rev. E **49**, 671 (1994).
[11] A. Proulx, A. Talebpour, S. Petit, and S.L. Chin, Opt. Commun. **174**, 305 (2000); S. Tzortzakis *et al.*, Opt. Lett. **27**, 1944 (2002); O.G. Kosareva *et al.*, *ibid.* **22**, 1332 (1997).
[12] C.-C. Cheng, E.M. Wright, and J.V. Moloney, Phys. Rev. Lett. **87**, 213001 (2001).
[13] G. Shvets, I. Kaganovich, and E. Startsev, Phys. Rev. Lett. **89**, 139301 (2002); V.T. Tikhonchuk, *ibid.* **89**, 209301 (2002).
[14] T.Zh. Esirkepov, Comput. Phys. Commun. **135**, 144 (2001); J. Villasenor and O. Buneman, *ibid.* **69**, 306 (1992).
[15] Z.M. Sheng, J. Meyer-ter-Vehn, and A. Pukhov, Phys. Plasmas **5**, 3764 (1998).
[16] L. Gorbunov, P. Mora, and T.M. Antonsen, Jr., Phys. Rev. Lett. **76**, 2495 (1996); N.E. Andreev, L.M. Gorbunov, V.I. Kirsanov, K. Nakajima, and A. Ogata, Phys. Plasmas **4**, 1145 (1997).
[17] U. Teubner *et al.*, Opt. Commun. **144**, 217 (1997); R. Lichters, Ph.D. thesis, Technical University München, 1997.